An Analytical Investigation of the Response of Steel Containment Models to Internal Pressurization

D.S. Horschel, T.E. Blejwas
Sandia National Laboratories, Division 9442, P.O. Box 5800, Albuquerque, New Mexico 87185, U.S.A.

SUMMARY

The response of experimental models of steel containment structures to pneumatic internal pressurization is being investigated as part of Sandia National Laboratories' Containment Integrity Program. This program is sponsored by the U.S. Nuclear Regulatory Commission. In this paper the finite element techniques and the results for the first two of three model configurations are discussed. The analyses using a preliminary stress-strain curve is compared to the updated analyses using the measured material properties.

The first configuration (baseline model) is a right circular cylinder welded to a hemispherical dome. The second configuration (ring stiffened model) is the same as the baseline model with ten stiffening rings added to the cylinder wall. The models, which are fabricated from very ductive low carbon steels, are expected to deform/strain significantly before failure; therefore, the finite element analyses include the effects of finite strains and geometric and material nonlinearities. A full Newton-Raphson technique and an updated Lagrangian formulation with follower forces are used in all of the analyses presented.

The material properties have a significant effect on containment model behavior due to static internal pressurization. When the preliminary stress-strain curve is used in the finite element analyses both models (baseline and ring stiffened) are able to carry a 30% increase in pressure after yielding; analyses using the actual measured material properties indicate that the increase in the pressure carrying capability of the models after yield is about 16%.

The baseline model is expected to fail in the cylindrical portion of the model. Failure of the ring stiffened model is expected to initiate in the rings and precipitate failure of the cylinder wall.

Experiments scheduled for completion in the first part of 1983 will be compared to the analytical predictions.

1. INTRODUCTION

As part of a combined analytical and experimental program on containment integrity at Sandia National Laboratories, experimental models of steel containment structures are being analyzed to predict their behavior during pneumatic internal pressurization to failure. The finite element analyses includes the effects of finite strains and geometric and material nonlinearities. From comparisons of current analyses with preliminary analyses [1], it is evident the form of the material stress-strain curve has a significant effect on containment behavior. The analyses are being compared with the experimental data as they become available; comparisons will be available for presentation at the SMiRT Conference. The experimental techniques and results will be in companion presentations [2,3]. A description of the overall program, which is sponsored by the U.S. Nuclear Regulatory Commission, is contained in Reference [4].

2. EXPERIMENTAL MODELS

Three steel model configurations, which are all right circular cylinders with an hemispherical dome, are being tested. The three configurations are:

1. Baseline configuration (no special features),
2. Ring stiffened model,
3. Baseline configuration with three penetrations.

A model that was built to develop fabrication procedures was tested at Sandia in December of 1982. This model, which was a baseline configuration, was used to check testing procedures and equipment. The testing program designed to investigate the behavior of the three model configurations is scheduled for completion in 1983.

The models are made from very ductile, low carbon steels. Materials used in actual steel containments have a higher carbon content with less ductililty (but still very ductile). These differences result in the significant change in the strain hardening slope and, consequently a change in the structural response of the models. The domes are formed using a spinning process. The cylinder is rolled from a flat sheet of steel, and has a welded vertical seam. The stiffening rings on the ring stiffened model will be brazed to the cylinder wall. The models are welded to a base ring which is in turn bolted to a very stiff testing fixture.

3. ANALYTICAL TECHNIQUES

3.1 General

The finite element analyses were performed using the J.1 and J.2 versions of the MARC code [5]. The analyses include material and geometric nonlinearities and finite strains. A full Newton-Raphson technique and an updated Lagrangian formulation with follower forces were employed in all of the analyses presented. The baseline configuration and the ring stiffened configuration were analyzed by taking advantage of axisymmetry. The analysis of the third configuration (baseline model with three penetrations) will be presented at a later date.

3.2 Preliminary Analyses

The preliminary analyses [1] were performed using estimated material properties and the dimensions that were specified in the construction drawings. All materials were assumed to have the same mechanical properties. A modulus of elasticity of 30,000,000 psi (207 GPa) and Poissons ration of 0.30 were assumed. The true stress-true strain curve shown in Figure 2 approximates SA 516 Gr 70 steel. A 0.15 (true) strain cut-off point was used in the analyses.

From preliminary analysis, the baseline model yields at about 140 psig (965 KPa) and reaches 0.15 strain at 185 psig (1276 KPa). The preliminary analysis of the ring stiffened model yielded at about 160 psig (1103 KPa) and reached 0.15 strain at 210 psig (1448 KPa). The radial displacement of a mid-height node in each of the containment models versus the analytically applied pressure as shown in Figure 3.

3.3 Current Efforts

The analyses of the baseline configuration and the ring stiffened containment have been redone using measured material properties. The elastic constants for the cylinder dome and ring materials were measured to be 30,500,000 psi (210 GPa) for the modulus of elasticity and 0.32 for Poissons ratio. The true stress-true strain curves for these materials are shown in Figure 4. The yield stresses of 40,000, 45,000 and 41,000 psi (276, 320 and 282 MPa) for the cylinder, dome and ring material, respectively, are lower than the yield stress used for the preliminary analyses. Also, the final strain hardening slope for each of these materials is much smaller than the strain hardening slope used in the preliminary analyses.

3.3.1 Baseline Configuration

The as-built dimensions were obtained for the baseline model and are compared to the specified dimensions in Table I. The large variation in the dome thickness is due to the spin forming process. The circumferential averages of the thickness for the dome at thirteen meridional locations are shown in Figure 5. A linear variation of thickness over the element length was used in the analysis.

The analytical model for the baseline configuration consists of 69 elements with 336 degrees of freedom. A four by four array of eight-node axisymmetric quadrilateral elements are used to impose a fixed boundary condition at the base. The remainder of the model consists of two-node axisymmetric cubic displacement shell elements. Eleven integration points are used through the thickness of the shell elements.

A general membrane yielding in the cylindrical section of the model is predicted to occur at about 92 psig (635 KPa). With a very small increase in the pressure, a large portion of the cylinder wall, displaces noticeably in the radial direction (bulging). This plastic flow with negligible pressure increase, which is due to the significant yield plateau in the cylinder wall material, was observed in the preliminary test.

The cylinder wall node with the maximum radial displacement plotted against applied pressure is shown in Figure 6. The maximum obtained plastic strain near the cylinder midheight plotted against applied pressure is shown in Figure 7. Comparing the plot of the displacement of midside node in the preliminary analyses (Figure 2) to Figure 6, the strain hardening slope significantly affects the ability of the structure to carry additional pressure after general yielding has been reached.

Although detailed data from the preliminary test of the check-out model are not available, a comparison of the observed and calculated displaced shapes (Figures 8a and 8b) is quite good. Note that the calculations used measurements of the baseline model, not the preliminary check-out model.

3.3.2 Ring stiffened Configuration

The finite element model for the ring stiffened model consists of 105 elements having a total of 490 degrees of freedom. As with the baseline model, the base is modeled with a four by four array of axisymmetric continuum elements. The remainder of the model consists of two-node cubic displacement shell elements. Each stiffening ring is represented by a single shell element. Again, eleven integration points are used through the thickness of the shell elements.

The ring stiffened model has not yet been fabricated, so the analysis uses the specified dimensions (Table II). It should be noted that the ring dimensions have been changed since the preliminary analysis. Due to fabrication problems and the possible buckling of the rings, narrower and thicker rings that bring the centroid closer to the shell wall were selected for model fabrication. The area of the new rings is about the same as that of the rings used in the preliminary analysis.

A general yielding of the cylinder wall of the ring stiffened model at about 116 psig (800 KPa) is predicted (about 26% higher than the baseline configuration). There is an 28% increase in the cylinder area of the ring stiffened model over the baseline model due to the addition of the rings and the slightly thicker wall. Because bending between rings does not increase noticeably after the cylinder wall yields, the rings will deform

plastically and displace an amount (nearly) equal to the cylinder wall to which it is attached. A displaced shaped for the ring stiffened model at 132.2 psig (911.5 KPa) is shown in Figure 9. Since the rings at this pressure level are near their ultimate strain level (0.17), failure of the model is imminent. The maximum plastic strain in the cylinder wall is about 0.020, with the maximum radial displacement being 3.9 inches. A plot of the pressure versus radial displacement of a node on the cylinder wall is shown in Figure 10.

4.0 CONCLUSIONS

The baseline model will yield at 92 psig (634 KPa). With an approximately 18% increase in the applied pressure, the cylinder wall will deform radially until the ultimate strain of the material is reached. The ring stiffened model will yield at 116 psig (800 KPa). With the pressure increased by about 14%, the rings will reach their ultimate capacity which will precipitate gross failure of the model. Although additional pressure carrying capability is desirable, the large displacements that are predicted for Sandia's models may not be obtainable in an actual containment due to piping constraints, shield-wall interactions or the effect of other details not included in the models.

5.0 FUTURE EFFORTS

The analysis of the ring stiffened model will be updated as soon as the model is measured. The thickness variations in the dome will be included as will the actual cylinder wall thicknesses. The third model configuration, i.e. the baseline configuration with three penetrations, will require a three dimensional analysis. The equipment hatch is of particular interest because the preliminary axisymmetric analyses indicated buckling at a pressure of about 120 psig (827 KPa) [1]. The results of these analyses will then be compared to the experimental results from Sandia's tests of the three model configurations.

This work is supported by the U.S. Nuclear Regulatory Commission, Office of Nuclear Regulatory Research, under Memorandum of Understanding DOE 40-550-75 with the U.S. Department of Energy.

REFERENCES

1. Blejwas, T. E.; Horschel, D. S. "Analysis of Steel Containment Models," Proceedings of the Workshop on Containment Integrity, NUREG/CP-0033, SAND82-1659, Arlington, Virginia, June 7-9, 1982.

2. Woodfin, R. L.; Dennis, A. W. "Techniques Used in Static Pneumatic Pressure Experiments on Models of a Generic Steel Containment Building," Proceedings Seventh Intl. Conference on Structural Mechanics in Reactor Technology, Chicago, Illinois, August 22-26, 1983, Paper J 6/3.

3. Woodfin, R. L.; Dennis, A. W. "Results Obtained from Static Pneumatic Pressure Experiments on Models of a Generic Steel Containment Building," Proceedings Seventh Intl. Conference on Structural Mechanics in Reactor Technology, Chicago, Illinois, August 22-26, 1983, Paper J 6/3.

4. Blejwas, T. E.; von Riesemann, W. A.; Costello, J. F., "The NRC Containment Integrity Program," Proceedings Seventh Intl. Conference on Structural Mechanics in Reactor Technology, Chicago, Illinois, August 22-26, 1983, Paper J 1/1.

5. MARC General Purpose Finite Element Program, MARC Analysis Research Corporation, Palo Alto, California, (1980).

TABLE I

Baseline Model Geometry

	SPECIFIED in. (mm)	MEASURED in. (mm)
Cylinder wall thickness	.0478 (1.214)	.040 to .045 (1.02 to 1.14)
Cylinder radius (inside)	21.56 (547.7)	21.59 to 21.61 (548 to 550)
Cylinder wall height	43.2 (1097)	43.2 (1097)
Dome wall thickness	.0478 (1214)	.038 to .072 (.963 to 1.831)

TABLE II

Ring Stiffened Model Geometry

	SPECIFIED (inches)	SPECIFIED (mm)
Cylinder wall thickness	.0478	1.214
Cylinder wall height	43.2	1097
Cylinder radius (inside)	21.562	547.7
Dome wall thickness	.0478	1.214
Ring radius (inside)	21.61	548.9
Ring radius (outside)	21.87	555.5
Ring thickness (height)	0.125	3.175

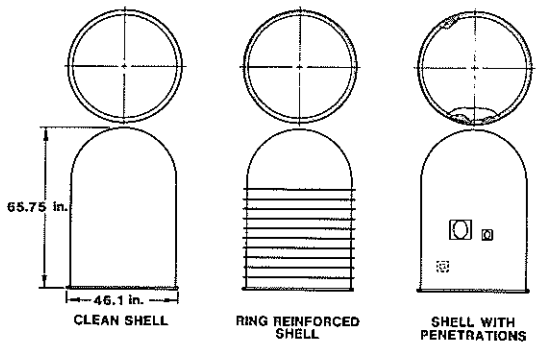

1. Experimental Model Configurations

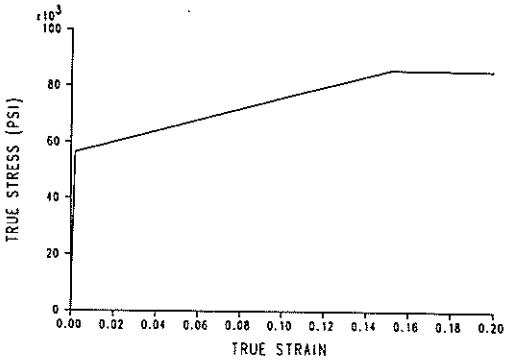

2. Preliminary True Stress-True Strain Curve

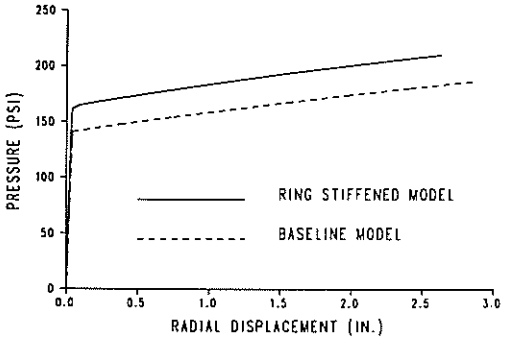

3. Pressures Versus Radial Displacement of Midside Nodes

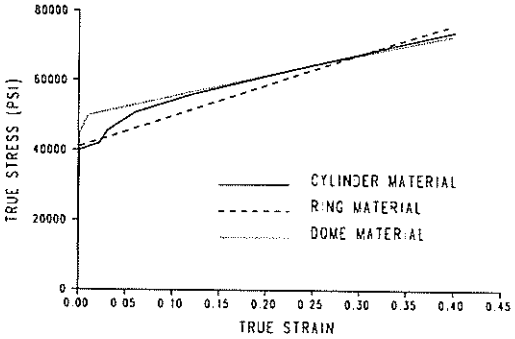

4. True Stress-True Strain Curve for the Model Materials

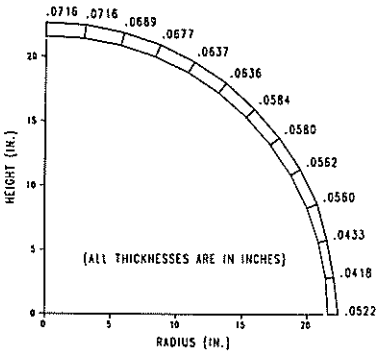

5. Dome Thickness for Baseline Model

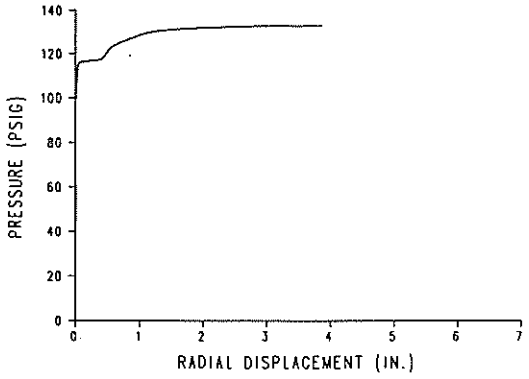

6. Pressure Versus Radial Displacement of a Cylinder Wall Node

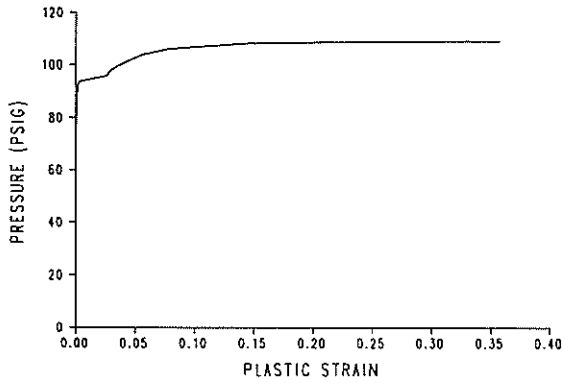

7. Pressure Versus Plastic Strain of a Cylinder Wall Gauss Point

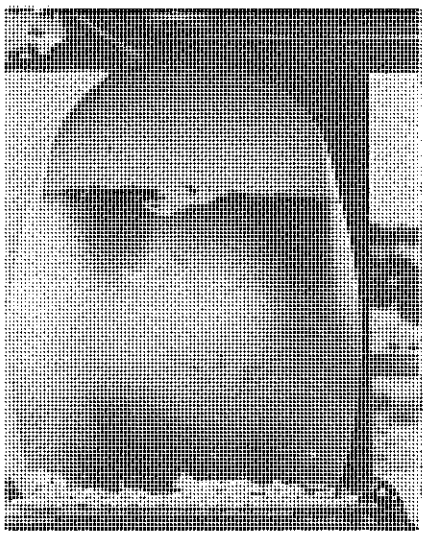

8a. Displaced Shape of the Check-Out Model

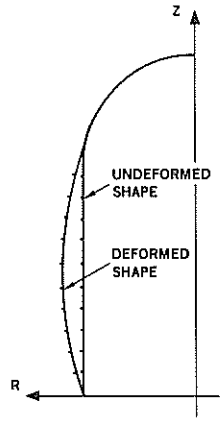

8b. Calculated displaced Shape of the Baseline Model

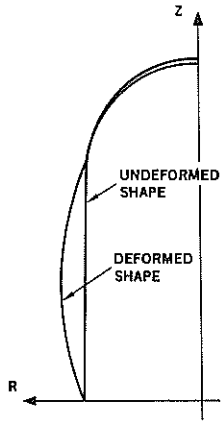

9. Displaced Shape of the Ring Stiffened Model

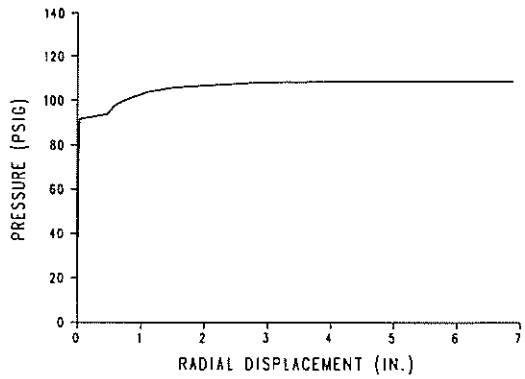

10. Pressure Versus Radial Displacement of a Cylinder Wall Node